Biochimica et Biophysica Acta 1848 (2015) 680–687

Contents lists available at ScienceDirect

Biochimica et Biophysica Acta

journal homepage: www.elsevier.com/locate/bbamem

# VCA1008: An Anion-Selective Porin of *Vibrio Cholerae*

Carolina L. Goulart [a,1], Paulo M. Bisch [b], Wanda M.A. von Krüger [b], Fabrice Homblé [a,*]

[a] Structure et Fonction des Membranes Biologiques, Centre de Biologie Structurale et de Bioinformatique, Faculté des Sciences, Université Libre de Bruxelles, Campus Plaine (CP 206/2), B - 1050 Brussels, Belgium

[b] Laboratório de Física Biológica, Instituto de Biofísica Carlos Chagas Filho, Universidade Federal do Rio de Janeiro, Rio de Janeiro, Brazil

ARTICLE INFO

*Article history:*
Received 15 August 2014
Received in revised form 5 November 2014
Accepted 10 November 2014
Available online 22 November 2014

*Keywords:*
porin
ion channel selectivity
Donnan potential

ABSTRACT

A putative porin function has been assigned to VCA1008 of *Vibrio cholerae*. Its coding gene, *vca1008*, is expressed upon colonization of the small intestine in infant mice and human volunteers, and is essential for infection. *In vitro*, *vca1008* is expressed under inorganic phosphate limitation and, in this condition, VCA1008 is the major outer membrane protein of the bacterium. Here, we provide the first functional characterization of VCA1008 reconstituted into planar lipid bilayers. Our main findings were: 1) VCA1008 forms an ion channel that, at high voltage (~ ± 100mV), presents a voltage-dependent activity and displays closures typical of trimeric porins, with a conductance of 4.28 ± 0.04 nS (n = 164) in 1M KCl; 2) It has a preferred selectivity for anions over cations; 3) Its conductance saturates with increasing inorganic phosphate concentration, suggesting VCA1008 contains binding site(s) for this anion; 4) Its ion selectivity is controlled by both fixed charged residues within the channel and diffusion along the pore; 5) Partitioning of poly (ethylene glycol)s (PEGs) of different molecular mass suggests that VCA1008 channel has a pore exclusion limit of 0.9 nm.



## 1. Introduction

The Gram-negative bacterium *Vibrio cholerae* can be found in aquatic environments, free-living or in association with phytoplankton, zooplankton, crustaceans and mollusks [1]. Several strains are facultative human pathogens that colonize the small intestine and cause cholera, an often fatal diarrheal disease [2]. Their ability to thrive in environments as distinct as the aquatic habitats and the human intestinal tract rests on a coordinately regulated gene expression to generate adaptive responses. For instance, the expression of genes encoding outer membrane proteins (OMP) can be differentially regulated by environmental cues, leading to alterations in the membrane properties, which contribute to the bacterial survival and adaptation to different niches [3,4]. As in other Gram-negative bacteria, diffusion of small molecules across the outer membrane of *V. cholerae* occurs through porins, which are transmembrane proteins folded in β-barrel structures [5,6].

*V. cholerae* El Tor biotype strain N16961 genome consists of two circular chromosomes of about 3.0 Mb and 1.0 Mb [7]. Most of OMP coding genes (*ompA*, *ompT*, *ompU*, *ompV*, *ompH*, *ompK* and *vc0972*) are found on the large chromosome, while three others (*ompW*, *ompS* and *vca1008*) are located in the small one. It is important to notice that the large chromosome harbors the majority of essential genes for cell functions and pathogenicity, whereas the small chromosome carries genes that appear to have origins other than the gamma-Proteobacteria [7]. The major porins of *V. cholerae* are OmpU and OmpT. Their distinct channel properties are related to resistance to bile salts [8] and to other membrane-destabilizing agents [9], as well as to organic acids tolerance [10]. Important roles in the physiology [11] and pathogenicity have also been assigned to other *V. cholerae* OMPs [12–14].

VCA1008, a novel *V. cholerae* OMP, was first described as an inorganic phosphate (Pi) starvation-induced protein, whose expression *in vitro* is dependent on the PhoB/PhoR system [15]. Disruption of *vca1008* led to growth defect, inability to colonize the intestinal tract of animal models and high susceptibility to sodium deoxycholate (DOC, the major bile compound) in the El Tor biotype strain N16961, but not in classical strain O395 of *V. cholerae* O1 [14]. Therefore, VCA1008 seems to have a strain-specific role in the physiology and pathogenicity of the bacterium. Furthermore, the absolutely requirement of VCA1008 for strain N16961 bile salt resistance *in vitro* is in perfect agreement with previous works showing that *vca1008* is expressed *in vivo* during infection and is essential for the intestinal colonization of infant mice and human volunteers by other El Tor strains [12,13,16]. Together, these results strongly indicate that VCA1008 plays important roles in the survival of *V. cholerae* El Tor strains in distinct environments.

Although it has been previously suggested that VCA1008 belongs to the bacterial porin family [14,15,17], experimental information about its function and structure is not available. Due to the importance of this protein for the physiology and pathogenicity of *V. cholerae*, we decided to investigate its electrophysiological properties. In this work, we demonstrated for the first time that VCA1008 inserts into artificial lipid bilayers as a homotrimer, where each monomer forms a channel with

* Corresponding author. Tel.: +32 2 650 5383; fax: +32 2 650 5382.
*E-mail address:* fhomble@ulb.ac.be (F. Homblé).
[1] Permanent address: Laboratório de Física Biológica†, Instituto de Biofísica Carlos Chagas Filho, Universidade Federal do Rio de Janeiro, Rio de Janeiro, Brazil.

http://dx.doi.org/10.1016/j.bbamem.2014.11.009
0005-2736/

preference for anions, and that its conductance is significantly affected by Pi concentration. In addition, our results suggest that VCA1008 selectivity is mainly due to the change in ion distribution between the solution and the inside of the channel.

## 2. Materials and Methods

### 2.1. Materials

The *Escherichia coli* polar lipid extract was purchased from Avanti Polar Lipid (Alabaster, AL) and octyl-POE (N-octylpolyoxyethylene) was obtained from Bachem (Bubendorf, Switzerland). Solutions were prepared with milli-Q water (Millipore Corporation, MA).

### 2.2. Strains and growth conditions

The strains used were *Escherichia* coli DH5α, SY327 λ*pir* and SM10 λ*pir* and *V. cholerae* wild type El Tor biotype, N16961 and its isogenic *ompU* mutant, CG7 (this work). Cells were routinely grown in rich medium LB (Lysogeny broth). For growth under defined Pi concentrations, TG medium (a mix of mineral salts and glucose buffered with Tris) was supplemented with $KH_2PO_4$, at 6.5 mM for high phosphate (HP), or at 65 μM, for low phosphate (LP) [18]. Bacterial growth was carried out in a 37°C shaking water-bath, at 200 rpm.

### 2.3. Genetic manipulations, cloning procedures and V. cholerae ompU mutant construction

A 1.0 kb fragment containing *ompU* gene was PCR amplified from *V. cholerae* N16961 genomic DNA using the primers OmpU-*Bam*HI (CCGGATCCCTGATTGCTCTTGCTGTATCAGC) and OmpU-*Hind*III (CAAGCTTGCCGATAGCCAGTTCGTCTTC). The amplicon was cloned into pGEM®-T Easy plasmid (Promega) according to supplier's recommendations to produce pGEM-ompU. This plasmid was digested with *Eco*RV within the *ompU* sequence, where a kanamycin resistance cassette, a 1.3 kb *Hinc*II fragment from pUC-4K [19] was inserted. Plasmid pGEM-ompU::Km was digested with *Eco*RI to remove the fragment containing the disrupted *ompU* sequence, which was then cloned into the *Eco*RI site in the suicide vector pGP704 [20], to generate pGP-ompU::Km. To facilitate *ompU* mutant selection, *sacB* gene (1.9 kb *Eco*RV/*Bam*HI fragment from pJG9 (J. Galen, unpublished data) was cloned into *Eco*RV/*Bgl*II-digested pGP-ompU::Km, yielding pGS3. Expression of the *Bacillus subtilis sacB* gene leads to sucrose sensitivity in most Gram-negative bacterial species [18]. For *V. cholerae* N16961 *ompU* selection using the allelic exchange strategy, *E. coli* strain SM10 λ*pir* transformed with pGS3 was used to mobilize the plasmid into *V. cholerae* N16961 by conjugation. A selection procedure on 5% sucrose allowed the isolation of the *ompU* exchange mutant, CG7, as previously described [18]. CG7 genotype was confirmed by PCR, Southern blot (data not shown) and SDS-PAGE analyses of outer membrane fractions.

### 2.4. Preparation of outer membrane fractions and VCA1008 purification

*V. cholerae ompU* mutant CG7 was cultivated in 500 mL of TGLP for 16 hours ($O.D._{600}$ 0.3) to allow *vca1008* expression. Cells were collected by centrifugation at 10,000 x g for 10 min at 4°C, resuspended in 6 mL of 20 mM Tris-HCl pH8.0 containing 1 mM PMSF and disrupted by sonication. Cell lysate was ultracentrifuged (70,000 x g for 40 min) and the insoluble fraction, containing cell membranes and debris, was washed twice with 6 mL of 1% sarkosyl in 20 mM Tris-HCl pH8.0, under similar condition. The final pellet was resuspended in 2 mL of 1% SB-12 in 20 mM Tris-HCl pH8.0 (buffer A) and ultracentrifuged at 70,000 x g for 1 hour. The supernatant containing soluble proteins was added to a DEAE-cellulose column, which was then washed with 100 mM NaCl in buffer A. Bound proteins were eluted using a 100-250 mM NaCl gradient in buffer A. Proteins in eluted fractions were analyzed by SDS-PAGE and Coomassie Blue stained. Protein concentration was determined using Bio-Rad Protein Assay Dye Reagent according to manufacturer's protocol.

### 2.5. Samples preparation and SDS-PAGE analysis

Cells were grown for 16 hours in 5 mL of TGHP or TGLP and then collected by centrifugation at 10,000 x g for 5 minutes (total $O.D._{600}$ of 0.5). The pellet was washed twice with PBS, suspended in 40 μL of SDS-PAGE loading buffer [1X] and incubated at 100°C for 5 minutes. The lysate was centrifuged as above, and a 7 μL aliquot of the supernatant was analyzed by SDS-PAGE. To investigate the proteins eluted from the DEAE-cellulose column, an aliquot of each eluate was mixed with equal volume of the SDS-PAGE loading sample buffer [2X], and the samples were treated as described above. To analyze the oligomeric state of VCA1008 purified by DEAE-cellulose chromatography, the mixture (1:1) of the eluate with the SDS-PAGE loading buffer [2X] was incubated for 5 minutes, at different temperatures, before the SDS-PAGE. Proteins were separated by SDS-PAGE on 11 or 12.5% polyacrylamide gels and bands were visualized by Coomassie blue staining.

### 2.6. Electrophysiology

Electrophysiological recordings were performed as described previously [21,22]. Briefly, VCA1008 protein purified by DEAE-cellulose chromatography was diluted in 1% octyl-POE and reconstituted into planar bilayers of *E. coli* polar lipids in hexane 2% (w/v), formed by the folding of two lipid monolayers over a hole (135 μm in diameter) in a 25 μm thick Teflon partition between the two Teflon experimental chambers. Before each experiment the partition was treated with a solution of hexane/hexadecane (2.5%, v/v) to increase its oleophylicity. Two Ag/AgCl electrodes, in series with a salt bridge (1M KCl in 1% agar), were used to connect the experimental chambers to the electronic equipment. The *trans* compartment was defined as the one connected to the ground and the voltage was applied to the *cis* compartment. Reconstitution of VCA1008 channel into the planar lipid bilayer was done by adding the protein to the *cis* compartment at a final concentration that varied from 0.2 to 20 ng/mL.

The current-voltage curve was acquired using a periodic symmetrical triangular voltage, 10 mHz in frequency, provided by a Wavetek 39 waveform generator (Wavetek, U.K.), and the current through the membrane was amplified by a BLM 120 amplifier (BioLogic, France). Data were filtered at 300Hz (5-poles linearized Tchebichev filter), digitized at 44.1 kHz with a DRA 200 interface (BioLogic, France) and stored on CDs using a homemade program written in the MATLAB environment (The MathWorks, Natick, MA), for further processing. The conductance was estimated in the linear part of the current-voltage curve around the reversal potential.

### 2.7. Determination of the channel ion selectivity

The reversal potential (zero-current potential) was set to zero in presence of identical salt concentration solution on both sides of the membrane. Then, the *cis* compartment was perfused three times its volume with a solution of different salt concentration and the change in reversal potential ($E^{rev}$) was recorded. The reversal potential was estimated experimentally by searching the membrane potential that cancel the membrane current and/or using the linear least square fitting of the current-voltage data. No significant difference was found between the two methods. The reversal potential was corrected for the liquid junction potential at the salt bridges, which was calculated using the liquid junction potential equation.

### 2.8. Determination of the effective pore size

The effective size limit of the VCA1008 pore was determined by solute exclusion, using neutral polyethylene glycols (PEGs) of discrete sizes, ranging from 68 to 6000 Da. VCA1008 was reconstituted into the lipid bilayer and its channel conductance was measured using the reference solution (1 M KCl buffered with 10 mM HEPES, pH7.5) on both sides of the membrane. Both *cis* and *trans* compartments were then perfused with the reference solution supplemented with 11% (wt/vol) of each PEG species used and the change in VCA1008 channel conductance was measured.

### 2.9. Statistics and data analysis

Data are shown as the mean ± standard error of the mean (n = number of experiments). Histogram of conductance was drawn and analyzed using GraphPad Prism v.5.0a. Nonlinear least square curve-fitting were performed under Matlab using the lsqcurvefit function.

## 3. Results

### 3.1. Conformational states and electrophoretic mobility of the purified native VCA1008

VCA1008 was purified by DEAE-cellulose chromatography from the outer membrane fraction of CG7 cells, grown in TGLP. Under this condition, CG7 major OMPs are OmpT and VCA1008 (Figs. 1SA and 1SB). These OMPs were eluted from the DEAE column at different concentrations of NaCl. Purified VCA1008 was eluted with NaCl between 200 and 250 mM and the final concentration of the stock solution was 0.17 mg $mL^{-1}$.

In a previous work [17], we showed that the VCA1008 from an outer membrane preparation of *V. cholerae* N16961 cells grown under Pi limitation, migrates across a denaturing polyacrylamide gel (0.1% SDS) as a high molecular complex (consistent with a trimer) when kept up to 50°C, but dissociated to monomeric species at 75°C. Similar temperature-induced conformational changes and migration behavior were observed when the native purified VCA1008 was incubated under low or high temperatures before electrophoresis (Fig. 1), indicating that VCA1008 expression in CG7 cells did not alter its oligomerization.

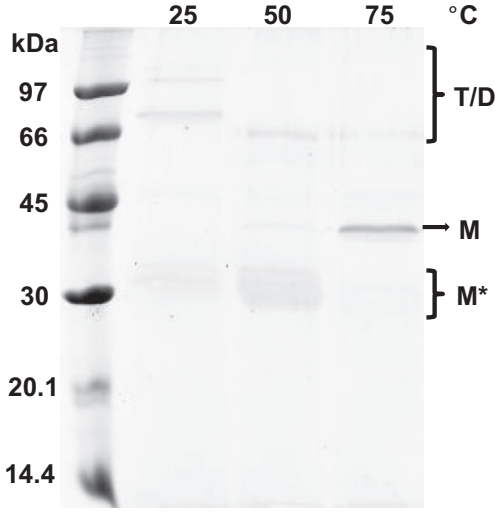


**Fig. 1.** Heat-induced conformational changes of native VCA1008 purified from *V. cholerae* N16961 cells cultivated in low Pi medium TGLP. The temperature effect on VCA1008 conformation was analyzed by SDS-PAGE 11% after protein incubation at 25°C, 50°C or 75°C for 5 minutes. The regions denoted with T/D, M or M* represent trimers and/or dimers, denatured monomers and folded monomers, respectively.

### 3.2. VCA1008 channel conductance and the trimeric state of the protein

The open conductance of VCA1008 channel was determined at +10 mV. At this voltage, the insertion of channels into the lipid bilayer yielded discrete current step increases in the same range of amplitude (Fig. 2A), indicating a sequential incorporation of a single protein channel unit into the bilayer.

The conductance distribution of individual current steps was fitted to a sum of two Gaussian **f**unctions and the maximum of each curve corresponds to the average conductance of a single channel unit (Fig. 2B).

In the presence of 1M KCl on both side of the membrane, about 85% of the channels reconstituted into the lipid bilayer had a reproducible unit conductance of 4.28 ± 0.04 nS (n = 164), whereas a minor fraction had a low conductance of 1.73 ± 0.07 nS (n = 30). The conductance of the large-conductance fraction is a nonlinear function of the KCl concentration. At high KCl concentration (≥0.5M) the magnitude of the conductance increased linearly with the salt concentration (Fig. 3). This linear dependence is a typical feature of large size β-barrel channels [5,23]. However, at low concentrations, the conductance is a nonlinear function of the KCl concentration. This nonlinearity is also observed when activity is used in place of the concentration (Fig. 2S), indicating that it is an intrinsic property of VCA1008.

Bacterial porins exist either in the monomeric (e.g., OmpA) or trimeric (e.g., OmpC and OmpF) form in the outer membrane [5]. Trimeric porins display a voltage-dependent activity at high voltages. More specifically, at voltages larger than ±100 mV each monomer closes independently giving rise to a stepwise decrease in the current [24,25]. Thus, to assess the voltage-dependence of the protein, a single unit of VCA1008 was reconstituted into the planar lipid bilayer and a triangular voltage wave was applied. As shown in Fig. 4A, discrete decreases in the

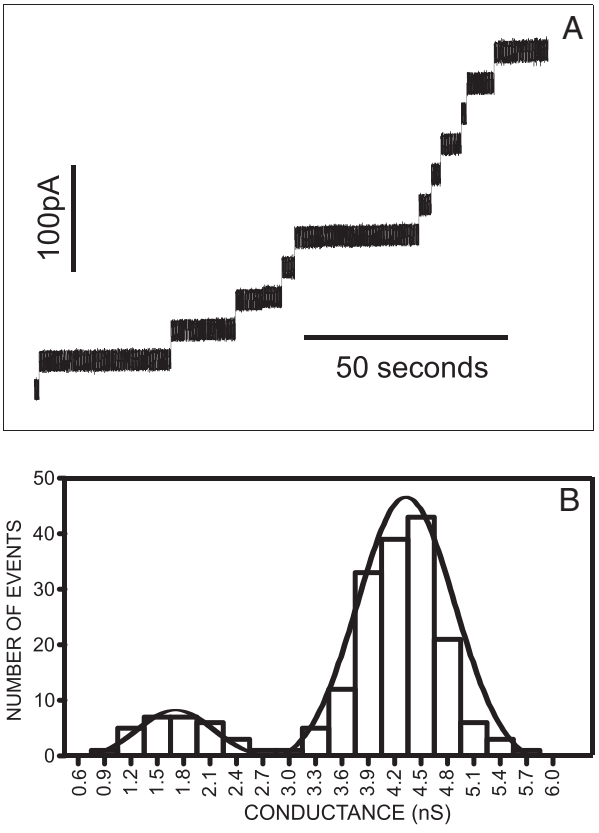


**Fig. 2.** Conductance of the VCA1008 channel. (A) Stepwise increase in the current through the lipid bilayer after sequential reconstitution of purified native VCA1008. The aqueous phase contained 1M KCl, 10 mM HEPES, pH7.5 and the applied voltage was +10 mV. (B) Conductances distribution of individual current steps. Data were fitted to a sum of two Gaussian curves ($R^2 = 0.984$).

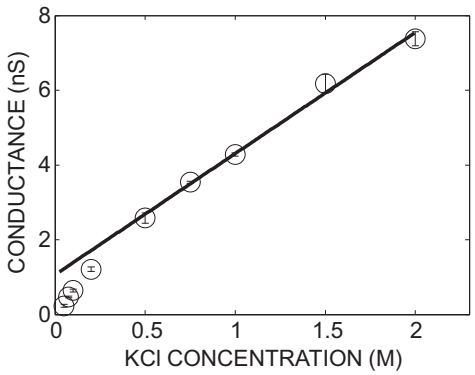


**Fig. 3.** Effect of KCl concentration on VCA1008 conductance. A single VCA1008 unit was reconstituted into a planar lipid bilayer formed from *E. coli* polar lipid by folding two monolayers. The aqueous phase contained KCl at different concentrations (50 mM to 2 M) in 10 mM HEPES, pH7.5. Data were fitted with a linear regression using conductance values obtained at high KCl concentration: from 0.5 to 2.0 molal ($r^2 = 0.993$).

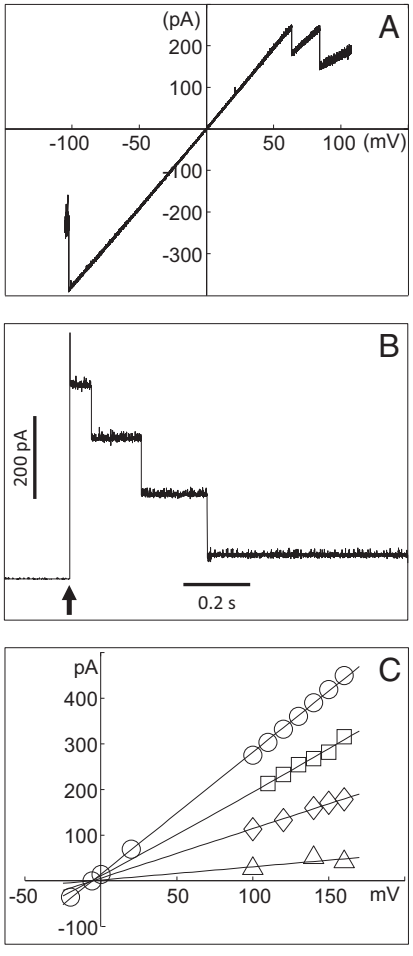


**Fig. 4.** Voltage dependence and ion selectivity of VCA1008 channel. (A) Current-voltage curve of a lipid bilayer showing closures at high positive or negative voltages (1 M KCl in 10 mM HEPES, pH7.5). (B) Change in the current flowing through a single VCA1008 trimer in response to a long lasting voltage of +120 mV (1 M KCl in 10 mM HEPES, pH7.5). The up arrow indicates the beginning of the voltage pulse. (C) The ionic selectivity of a single trimeric VCA1008 unit was measured in the presence of a twofold KCl gradient (1/0.5 M; *trans*/*cis*) and the different conductance levels were observed. The *trans* compartment was connected to the ground. Thus, a negative reversal potential indicates a preference for anions over cations. The reversal potential equals -6mV for all conductance levels: circle = trimer conductance, square = dimer conductance, diamond = monomer conductance and triangle = closed state. Data were fitted by a linear least squared procedure (goodness of the fit regression: $R^2 > 0.999$).

current through the membrane occurred around ±100 mV indicating channel closures.

To determine the oligomeric state of a single VCA1008 unit reconstituted into the bilayer, the successive closures of its channels were recorded during a long lasting high voltage step. We observed that the closures occurred in three steps of similar amplitude, which is typical of bacterial porins [26]. As each closure step corresponds to a decrease of about 1/3 of the total pore conductance (Fig. 4B), we suggest that the VCA1008 unit is formed by three monomers of the protein.

### 3.3. Ionic selectivity of the VCA1008 channel

To assess the ion selectivity of VCA1008, a single VCA1008 trimer was reconstituted into a lipid bilayer in symmetric KCl 1M solutions and the characteristic current-voltage curve was recorded after perfusing the *cis* compartment with 0.5 M KCl (Fig. 4C).

The different I/V curves correspond to the distinct open conformations of the protein VCA1008 in the lipid bilayer (trimeric, dimeric, monomeric and closed state), in the presence of a twofold KCl gradient (1/0.5 M; *trans*/*cis*). A linear regression through the data series shows that they all cross the abscissa at the same reversal potential value ($E^{rev}$), thus indicating that each monomer had the same ionic selectivity (Fig. 4C).

The interpretation of the $E^{rev}$ in terms of selectivity is model dependent. To perform a quantitative analysis of the selectivity, the $E^{rev}$ was measured in the presence of different concentration gradients across the membrane. The *trans* compartment was fixed at 1 M KCl, and the salt concentration in the *cis* compartment varied from 1 M to 25 mM KCl. In all cases, a negative shift in reversal potential was observed, indicating that the VCA1008 channel has a preference for anions over cations (Fig. 5). The reversal potential decreased monotonically at least up to a concentration ratio, $r = C_{trans}/C_{cis}$, of 40.

To have a first insight into the origin of the ionic selectivity of VCA1008 we used two macroscopic electrodiffusion models that assume independent movement of ions. The first model assumes a local electroneutrality along the channel. The zero-current potential ($E^{Planck}$) is given by the Planck equation (1)):

$$E^{Planck} = \frac{RT}{F}\frac{D_A - D_C}{z_A D_A - z_C D_C} \ln \frac{C^{trans}}{C^{cis}} \quad (1)$$

Where R is the gas constant, T is the absolute temperature, F is the Faraday constant, z is the ionic charge, D is the diffusion coefficient, $C^{trans}$ and $C^{cis}$ are concentrations of ion species and the subscripts A and C refer to anions and cations, respectively. This electric potential difference is the one that will be set up across a neutral channel in the

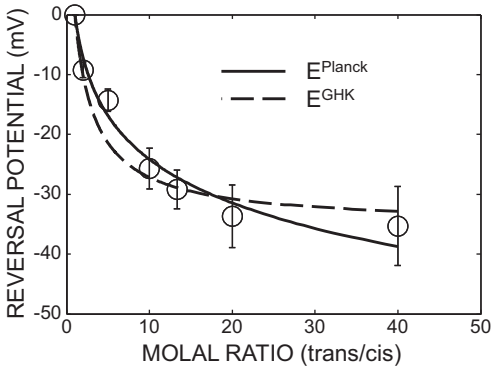


**Fig. 5.** Reversal potential of VCA1008 as a function of KCl concentration ratio $C^{trans}/C^{cis}$. The *trans* compartment KCl concentration was fixed at 1 M while the salt concentration in the *cis* compartment varied. A nonlinear least square regression was used to fit the data to either the GHK equation (dashed line) ($P_{Cl}/P_K = 4.01$, goodness of the fit regression: $R^2 = 0.959$) or the Planck diffusion equation (continuous line) ($D_{Cl}/D_K = 2.42$, goodness of the fit regression: $R^2 = 0.983$).

presence of a salt gradient due to the fact that different ions have distinct diffusion coefficients in solution.

The second model is the well-known Goldman-Hodgkin-Katz (GHK), which assumes a constant electric field along the channel [27]. For a symmetric monovalent salt the zero-current GHK potential ($E^{GHK}$) is given by:

$$E^{GHK} = \frac{RT}{F} ln \frac{\alpha C_C^{trans} + C_A^{cis}}{\alpha C_C^{cis} + C_A^{trans}} \quad (2)$$

where R is the gas constant, T is the absolute temperature, F is the Faraday constant, $\alpha$ is the permeability ratio ($P_C/P_A$), $C_{A,C}^{trans}$ and $C_{A,C}^{cis}$ are the bulk concentration of ion species (subscripts A and C refer to anions and cations, respectively) in the *trans* and *cis* compartments. As shown in Fig. 5 the best fit of the experimental data was obtained with the Planck equation (continuous line). This result is at odds with experimental and theoretical studies showing the role of charged residues on the ionic selectivity of β-barrel channels, such as those of the *E.coli* porin OmpF [28,29], the mitochondrial VDAC [30–32] as well as nanopores [33]. Thus, a plausible explanation for the Planck equation to best fit the data in Fig. 5 is the relatively high KCl concentration (the *trans* side being fixed at 1 M) used in these experiments that might screen the electrostatic effect of charged residues.

To assess the effect of charged residues inside the pore on the reversal potential we performed experiments at different KCl concentrations keeping the concentration ratio constant (Fig. 6). According to Planck equation, $E^{rev}$ should be constant as it depends on the concentration ratio, but not on the absolute salt concentration. However, we observed that $E^{rev}$ is a nonlinear function of the absolute concentration of KCl. Its value is about -2 mV at high absolute concentration and becomes more negative as the absolute concentration decreases, in agreement with an electrostatic screening of the charged residues.

To consider the role of the fixed charges, we resort to the Theorell-Meyer-Sievers (TMS) theory [34], which posits a Donnan equilibrium at each open end of the channel in series with the electrodiffusion of ions inside the pore. The Donnan equilibrium describes the ions partition at a channel-solution interface due to the effective charge in the channel. Consequently, a Donnan potential ($E^{Donnan}$) would occur in series with the diffusion potential ($E_{rev}^{Planck-FC}$) across the channel, accounting for the distribution of effective fixed charges that prevails inside the diffusion pore. Thus, for diffusion pores of nanometric diameters the reversal potential would be given by:

$$E_{rev}^{TMS} = E_{trans}^{Donnan} + E_{rev}^{Planck-FC} - E_{cis}^{Donnan} \quad (3)$$

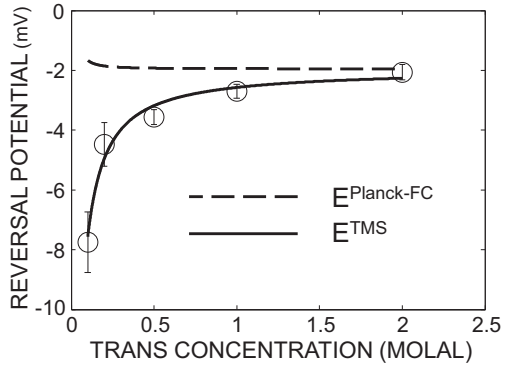


**Fig. 6.** Effect of ionic strength on the reversal potential of VCA1008 channel at a fixed concentration ratio *trans*/*cis* = 2. A nonlinear least square regression was used to fit the data to TMS model (Eq. (6)) (continuous line) ($D_{Cl}/D_K = 1.25$, effective fixed charge concentration $\overline{X} = 0.05$ M, goodness of the fit $R^2 = 0.983$). The contribution of $E_{rev}^{Planck-FC}$ to the total reversal potential is close to zero (dashed line).

The negative sign on the right side of the equation (3) arises from the fact that the two Donnan potentials are opposite in direction. The Donnan potential is given by:

$$E^{Donnan} = \frac{RT}{F} \ln r \quad (4)$$

where r is the Donnan ratio (viz., the ratio between the concentrations in the bulk and inside the channel: $r = (C_{channel}/C_{bulk})^{1/z}$, and z is the charge of the ion), which depends on the channel fixed charge and on the ion concentration (more accurately ion activity) in the bulk solution:

$$r = -\frac{\omega \overline{X}}{2C_{bulk}} + \sqrt{1 + \left(\frac{\omega \overline{X}}{2C_{bulk}}\right)^2}, \quad (5)$$

where ω is the sign of the channel fixed charge and $\overline{X}$ its concentration. Thus, inserting equations (4) and (5) into equation (3) gives:

$$E_{rev}^{TMS} = \frac{RT}{F} ln \frac{r_{cis}}{r_{trans}} + \frac{RT}{F} \frac{D_{Cl} - D_K}{z_{Cl} D_{Cl} - z_K D_K} ln \frac{D_K \bar{C}_K^{trans} + D_{Cl}\left(\bar{C}_K^{trans} + \omega \overline{X}\right)}{D_K \overline{C}_K^{cis} + D_{Cl}\left(\overline{C}^{cis}{}_k + \omega \overline{X}\right)}, \quad (6)$$

where $\overline{C}_j^{trans}$ *and* $\overline{C}_j^{cis}$ are the concentration of ion species j inside the channel on the *trans* and *cis* side. The second term on the right side is the Planck equation that takes into account the fixed charges within the channel. The relationship between the reversal potential of the VCA1008 channel and the ratio of the symmetrical monovalent salt concentrations in the compartments *trans*/*cis*, shown in Fig. 6, correctly fitted equation (6). At high KCl concentration the $E_{rev}^{TMS}$ is close to the diffusion potential ($E_{rev}^{Planck-FC}$), indicating the screening of the effective positive charges by counter-ions. As the concentration lowers the counter-ions screening effect weakens and the $E_{rev}^{TMS}$ diverges from the diffusion potential, highlighting the contribution of the effective fixed charge.

### 3.4. Effect of Pi on VCA1008 reversal potential and channel conductance

VCA1008 is synthesized when *V. cholerae* cells are grown *in vitro* under phosphate limitation (65 μM $KH_2PO_4$) [15]. This prompted us to investigate the effect of Pi on the VCA1008 channel selectivity and conductance. For the sake of comparison with KCl, the $KH_2PO_4$ solutions were prepared at pH 5.0, since at this pH each molecule is a monovalent salt and thus their anions have the same charge. The data presented in the previous section were collected in KCl at pH 7.5. A possible effect of pH change in the reversal potential was tested in KCl, but no difference was observed (Fig. 7A). However, in 0.1 M $KH_2PO_4$ the reversal potential decreased four fold, indicating a much lesser preference of VCA1008 for the anion (Fig. 7A). The conductance of the trimeric VCA1008 in 0.1 M $KH_2PO_4$ (0.84 ± 0.16 nS, n = 4) compared to that in KCl (0.64 ± 0.07 nS, n = 5) indicated that there is no significant difference between them (p = 0.18, t-test). However, in contrast to the results observed with KCl (Fig. 3), the VCA1008 channel conductance showed dependence on $KH_2PO_4$ concentration, and saturated above 1M (Fig. 7B). These results appear to violate the principle of independence of ion movement assumed in the Planck and GHK equations. The line drawn through the data in Fig. 7B is the best fit of the data to an empirical hyperbolic equation:

$$g = \frac{g_{max}\,[KH_2PO_4]}{[KH_2PO_4] + K_{0.5}}, \quad (7)$$

where g is the channel conductance, $g_{max}$ its maximal value, $[KH_2PO_4]$ is the concentration (pH 5.0), and $K_{0.5}$ is the concentration at half-maximal conductance. Since the conductivity of a $KH_2PO_4$ solution varied linearly within the concentration range used in this study,

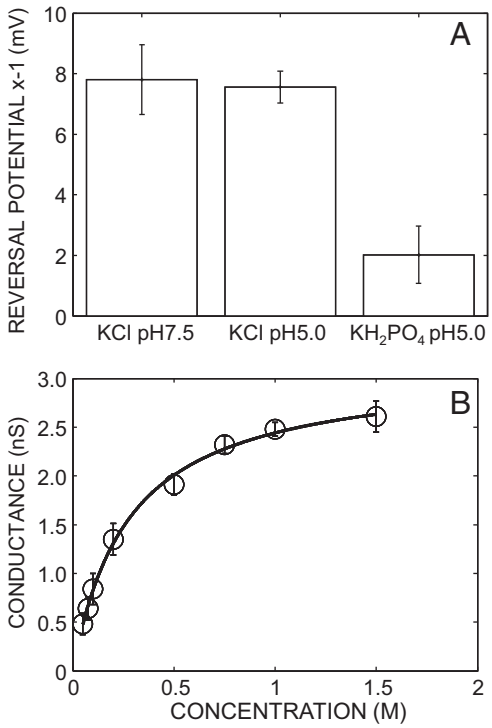


**Fig. 7.** Effect of pH and phosphate on the reversal potential and VCA1008 channel conductance. (A) The reversal potential was measured using a $KH_2PO_4$ concentration ratio equal to 2 [100 mM/50 mM, (*trans*/*cis*)]. (B) Concentration dependence of VCA1008 channel conductance measured in symmetrical $KH_2PO_4$ concentration from 50 mM to 1.5 M (pH 5.0). The plot has been fitted with a Langmuir isotherm of the form: $g = g_{max}/(1 + K_{0.5}/[C])$, where g is the channel conductance, $g_{max}$ (3.12 nS) is the asymptotic value, [C] is the $KH_2PO_4$ concentration (pH 5.0), and $K_{0.5}$ (0.28 M) is the concentration at which $g = g_{max}/2$ using a nonlinear least square iteration procedure (goodness of the fit regression: $R^2 = 0.998$).

the saturation effect (Fig. 7B) is likely to arise from an ion-channel interaction during ion translocation along the pore. The $K_{0.5}$ value (0.28 M) is two orders of magnitude higher than the phosphate concentration found in the small intestine where *V. cholerae* inhabits during infection. As the non-ideality of the $KH_2PO_4$ solution is relatively strong we also plotted the conductance as a function of the $KH_2PO_4$ activity (Fig. 3S). This result also features saturation but in this case the $K_{0.5}$ was twice (0.3 activity = 0.6 M) larger than that calculated using the molal concentration.

### 3.5. Size of VCA1008 channel pore

The pore size of a channel can be estimated by a polymer-induced change in the channel conductance [35]. Molecules smaller than the pore diameter can enter the channel and reduce its conductance, whereas molecules larger than the pore size will have little effect on the channel conductance. We examined the size exclusion limit of a single VCA1008 trimer in the absence and in the presence of PEGs (11 %) of different molecular mass, added on both sides of the lipid bilayer. PEGs are neutral polymers, almost spherical in aqueous solutions, whose hydrodynamic radii are known and are proportional to their molecular mass. They have been widely used to measure the effective diameter of channel pores [36,37]. We used PEGs ranging from 62 to 6000 Da and estimated the change in the VCA1008 channel conductance [$g(\omega)$] relative to its conductance in PEG free solution ($g_0$). Fig. 8 summarizes conductance measurements for the range of PEG sizes used, showing that the dependence of a PEG-induced channel conductance change on the polymer molecular weight is sigmoidal.

Small PEGs (<200 Da) permeated the channel and decreased its conductance to a value close to that of the PEG-free solution, whereas large

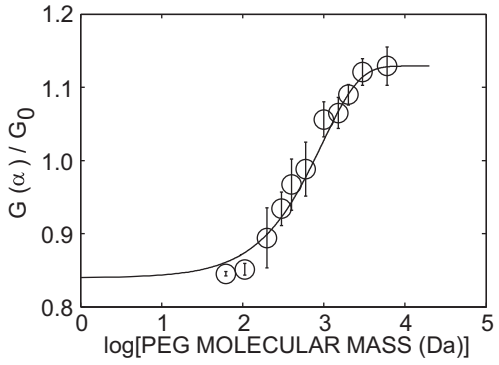


**Fig. 8.** The relative changes in single VCA1008 trimer conductance as a function of the PEG molecular mass. VCA1008 trimer conductance was measured in the absence and in the presence of PEGs (11 %) of different molecular mass, on both sides of the bilayer. The ordinate is the ratio of the fully open trimer conductance measured in the presence of PEG over the conductance measured without PEG. The data were measured in 1 M KCl and fitted to $g(\omega)/g_0 = 1 - \chi \exp(-(\omega/\omega_0)^{\alpha})$ with $\chi = 0.29$, $\alpha = 0.94$, and $\omega_0 = 950$ using a nonlinear least square iteration procedure (goodness of the fit regression: $R^2 = 0.998$).

PEGs (≥3000 Da) did not partition between the solution and the VCA1008 channel (Fig. 8). The effect of intermediately sized PEGs (200 to 2000 Da) on VCA1008 channel conductance was inversely proportional to their sizes. The presence of the impermeant PEG (above 1000 Da) resulted in a conductance higher than in PEG-free, which is indicative of an increased KCl activity inside the channel due to binding of water molecules to PEG [38,39].

Assuming that the polymer/weight-dependent reduction in the porin conductance is proportional to the polymer partition coefficient, the data of Fig. 7 can be fitted to the following equation [40,41]:

$$g(\omega)/g_0 = 1 - \chi \exp(-(\omega/\omega_0)^{\alpha}) \quad (8)$$

where $\chi$ represents the relative amplitude of the conductance of the channel between a regime where PEGs are fully excluded and a regime where they fully enter the pore, $\alpha$ represents the steepness of the transition between the regimes of full exclusion and full inclusion, and $\omega_0$ is the cut-off molecular weight for PEG. The solid line in Fig. 7 show the result of fitting that yield, $\chi = 0.29$, $\alpha = 0.94$, and $\omega_0 = 950$. An effective molecular weight of 950 corresponds to a PEG hydrodynamic radius of 0.92 nm [35].

## 4. Discussion

Bacterial porins are outer membrane spanning proteins that form aqueous channels allowing the passage of small solutes measuring up to about 600 Da [5]. OmpU and OmpT are the major porins in *V. cholerae* cells grown under standard conditions (LB medium, 37°C). They are both cation-selective porins and their channel properties have been characterized in detail [42–45]. In this work, we characterized the first anion-selective porin of *V. cholerae* ever described and we showed that its selectivity is consistent with its presumed role in phosphate acquisition, under phosphate starvation. This is similar to PhoE and OprP from *E. coli* and *P. aeruginosa* which are also expressed under phosphate starvation conditions [46–49].

However, the electrophysiological properties of VCA1008 from *V. cholerae* are significantly different from those of PhoE and OprP. For instance, in KCl solution VCA1008 has a conductance and an anion selectivity about twice as large as those of PhoE [50–52]. OprP has a conductance 5 times lower than VCA1008 but it is nearly perfectly selective to anions [53–55].

Both electrophoretic patterns and electrophysiology data indicated that VCA1008 is trimeric, like many other ion translocating bacterial porins. Unheated native VCA1008 protein migrates in a

polyacrylamide gel as a high molecular weight complex, which, when reconstituted into a planar lipid bilayer, forms voltage-dependent channels that closes in three steps of equal amplitude, indicating it contains three pores of identical conductance. Moreover, each monomer has the same ion selectivity suggesting that VCA1008 is a homotrimer.

PEG partitioning experiments suggested a size exclusion limit for the VCA1008 pore corresponding to a polymer hydrodynamic radius of 0.9 nm, which is consistent with those of *E. coli* OmpF from (1.0nm) [41] and *Borrelia burgdorferi* P66 (0.94nm) [37], estimated using the same method.

OmpF, a cation selectivity outer membrane porin of *E. coli*, whose structure is known at the atomic level, has been extensively used as a model protein for the study of the ionic selectivity of porins [28,42,56]. Those studies and others, using both theoretical and experimental analyses, highlighted the role of protein channel fixed charge density on its ionic selectivity process [31,57–60]. They also indicated that selectivity through nanosized ion channels is determined by the distribution of ions between the diffusion pore and the bulk electrolytic solution, and by the differences in ion mobility within the pore [28]. Such observations prompted us to use the macroscopic electrostatic Donnan equilibrium model and the diffusive process to describe the VCA1008 ionic selectivity. The usefulness of this approach has already been shown, notably to explain the behavior of bacterial porins ionic selectivity, at least in the limit of its approximations [56]. Unfortunately, it does not provide an accurate description of the channel ion selectivity but allow us to grasp, at least qualitatively, the basis of the selectivity process. Precise quantitative analyses of the ion concentration effects on the reversal potential would require the knowledge of the protein structure at the atomic resolution. The reversal potential values of VCA1008 showed that it is more selective to anions than cations. At a constant salt concentration ratio across the membrane, the cation selectivity of VCA1008 increased when the absolute value of the concentration decreased. This might be understood as a direct consequence of the charged residue distribution within the diffusion pore. More specifically, at low ionic concentration the screening of the fixed charge in the channel might be less efficient and the Donnan effect would increase. Electrostatic-dependent ion channel selectivity is a typical feature of β-barrel transmembrane proteins with nanosized diffusion pores such as those of bacterial porins, mitochondrial VDAC and synthetic nanopores [31,32,61].

The nonlinear dependence of the conductance on the concentration (activity) is also a consequence of the electrostatic Donnan equilibrium. At low concentration, the electric field created by the net charge inside the channel increases the ion concentration inside the channel. This effect decreases exponentially with the increase in concentration. At sufficiently high concentration, the electrostatic effect of the fixed charges is screened by counter ions. Thus, the channel behaves like a neutral pore and the ion concentration inside the channel is proportional to that in the external concentration.

At pH 5.0, $KH_2PO_4$ exists predominantly as monovalent phosphate anion, $H_2PO_4^-$. Thus, the difference between the effect KCl and $KH_2PO_4$ on the concentration-conductance relationship should be due to the anion. Therefore, the conductance saturation observed in the presence of the phosphate salt might indicate the presence of binding site (s) for the anion within the VCA1008 channel, Assuming that the number of binding sites is limited [62], the ion flux through the channel will not be proportional to the ion concentration, since binding hinders the translocation of ions through the channel.

In summary, in this study we demonstrated that VCA1008 is a new porin of *V. cholerae*, which displays a typical trimeric gating behavior, is more selective for monovalent anions than cations and has putative binding site(s) for phosphate. Moreover, its selectivity is mainly governed by the fixed charges of the basic residues lining the channel.

## Acknowledgments

FH is a Research Director at the FRS-FNRS (Belgium). CG was a recipient of the financial support from CNPq and CAPES (Brasil).

## Appendix A. Supplementary data

Supplementary data to this article can be found online at http://dx.doi.org/10.1016/j.bbamem.2014.11.009.

## References

[1] S.N. Wai, Y. Mizunoe, S. Yoshida, How Vibrio cholerae survive during starvation, FEMS Microbiol. Lett. 180 (1999) 123–131.
[2] J.B. Kaper, J.G. Morris Jr., M.M. Levine, Cholera, Clin. Microbiol. Rev. 8 (1995) 48–86.
[3] J. Lin, S. Huang, Q. Zhang, Outer membrane proteins: key players for bacterial adaptation in host niches, Microbes Infect. 4 (2002) 325–331.
[4] H. Nikaido, Microdermatology: cell surface in the interaction of microbes with the external world, J. Bacteriol. 181 (1999) 4–8.
[5] H. Nikaido, Molecular basis of bacterial outer membrane permeability revisited, Microbiol. Mol. Biol. Rev. 67 (2003) 593–656.
[6] A.H. Delcour, Solute uptake through general porins, Front. Biosci. 8 (2003) d1055–d1071.
[7] J.F. Heidelberg, J.A. Eisen, W.C. Nelson, R.A. Clayton, M.L. Gwinn, R.J. Dodson, D.H. Haft, E.K. Hickey, J.D. Peterson, L. Umayam, S.R. Gill, K.E. Nelson, T.D. Read, H. Tettelin, D. Richardson, M.D. Ermolaeva, J. Vamathevan, S. Bass, H. Qin, I. Dragoi, et al., DNA sequence of both chromosomes of the cholera pathogen Vibrio cholerae, Nature 406 (2000) 477–483.
[8] D. Provenzano, K.E. Klose, Altered expression of the ToxR-regulated porins OmpU and OmpT diminishes Vibrio cholerae bile resistance, virulence factor expression, and intestinal colonization, Proc. Natl. Acad. Sci. U. S. A. 97 (2000) 10220–10224.
[9] J. Mathur, M.K. Waldor, The Vibrio cholerae ToxR-regulated porin OmpU confers resistance to antimicrobial peptides, Infect. Immun. 72 (2004) 3577–3583.
[10] D.S. Merrell, C. Bailey, J.B. Kaper, A. Camilli, The ToxR-mediated organic acid tolerance response of Vibrio cholerae requires OmpU, J. Bacteriol. 183 (2001) 2746–2754.
[11] J. Reidl, K.E. Klose, Vibrio cholerae and cholera: out of the water and into the host, FEMS Microbiol. Rev. 26 (2002) 125–139.
[12] C.G. Osorio, H. Martinez-Wilson, A. Camilli, The ompU Paralogue vca1008 is required for virulence of Vibrio cholerae, J. Bacteriol. 186 (2004) 5167–5171.
[13] C.G. Osorio, J.A. Crawford, J. Michalski, H. Martinez-Wilson, J.B. Kaper, A. Camilli, Second-generation recombination-based in vivo expression technology for large-scale screening for Vibrio cholerae genes induced during infection of the mouse small intestine, Infect. Immun. 73 (2005) 972–980.
[14] C.L. Goulart, G.G. dos Santos, L.C. Barbosa, L.M. Lery, P.M. Bisch, W.M. von Kruger, A ToxR-dependent role for the putative phosphoporin VCA1008 in bile salt resistance in Vibrio cholerae El Tor N16961, Microbiology 156 (2010) 3011–3020.
[15] W.M. von Kruger, L.M. Lery, M.R. Soares, F.S. de Neves-Manta, C.M. Batista e Silva, A.G. Neves-Ferreira, J. Perales, P.M. Bisch, The phosphate-starvation response in Vibrio cholerae O1 and phoB mutant under proteomic analysis: disclosing functions involved in adaptation, survival and virulence, Proteomics 6 (2006) 1495–1511.
[16] M.J. Lombardo, J. Michalski, H. Martinez-Wilson, C. Morin, T. Hilton, C.G. Osorio, J.P. Nataro, C.O. Tacket, A. Camilli, J.B. Kaper, An in vivo expression technology screen for Vibrio cholerae genes expressed in human volunteers, Proc. Natl. Acad. Sci. U. S. A. 104 (2007) 18229–18234.
[17] C.L. Goulart, L.M.S. Lery, M.M.P. Diniz, J.L. Vianez, A.G.C. Neves-Ferreira, J. Perales, P.M. Bisch, W.M.A. von Kruger, Molecular analysis of VCA1008: a putative phosphoporin of Vibrio cholerae, FEMS Microbiol. Lett. 298 (2009) 241–248.
[18] W.M. von Kruger, S. Humphreys, J.M. Ketley, A role for the PhoBR regulatory system homologue in the Vibrio cholerae phosphate-limitation response and intestinal colonization, Microbiology 145 (Pt 9) (1999) 2463–2475.
[19] A. Oka, H. Sugisaki, M. Takanami, Nucleotide sequence of the kanamycin resistance transposon Tn903, J. Mol. Biol. 147 (1981) 217–226.
[20] V.L. Miller, J.J. Mekalanos, A novel suicide vector and its use in construction of insertion mutations: osmoregulation of outer membrane proteins and virulence determinants in Vibrio cholerae requires toxR, J. Bacteriol. 170 (1988) 2575–2583.
[21] F. Homblé, L. Mlayeh, M. Léonetti, Planar Lipid Bilayers for Electrophysiology of Membrane-Active Peptides, in: M.A.R.B. Castanho (Ed.), Membr. Pept. Methods Results Struct. Funct. International University Line, La Jolla, 2010, pp. 281–320.
[22] L. Mlayeh, S. Chatkaew, M. Leonetti, F. Homblé, Modulation of plant mitochondrial VDAC by phytosterols, Biophys. J. 99 (2010) 2097–2106.
[23] S. Pezeshki, C. Chimerel, A.N. Bessonov, M. Winterhalter, U. Kleinekathofer, Understanding ion conductance on a molecular level: an all-atom modeling of the bacterial porin OmpF, Biophys. J. 97 (2009) 1898–1906.
[24] J.H. Lakey, F. Pattus, The voltage-dependent activity of Escherichia coli porins in different planar bilayer reconstitutions, Eur. J. Biochem. 186 (1989) 303–308.
[25] B. Dargent, W. Hofmann, F. Pattus, J.P. Rosenbusch, The selectivity filter of voltage-dependent channels formed by phosphoporin (PhoE protein) from E coli, EMBO J. 5 (1986) 773–778.
[26] A.H. Delcour, Structure and function of pore-forming β-barrels from bacteria, J. Mol. Microbiol. Biotechnol. 4 (2002) 1–10.
[27] B. Hille, Ionic Channel of Excitable Membranes, Sinauer Associates, Sunderland, 1992.

[28] A. Alcaraz, E.M. Nestorovich, M. Aguilella-Arzo, V.M. Aguilella, S.M. Bezrukov, Salting out the ionic selectivity of a wide channel: the asymmetry of OmpF, Biophys. J. 87 (2004) 943–957.
[29] W. Im, B. Roux, Ion permeation and selectivity of OmpF porin: a theoretical study based on molecular dynamics, Brownian dynamics, and continuum electrodiffusion theory, J. Mol. Biol. 322 (2002) 851–869.
[30] E.B. Zambrowicz, M. Colombini, Zero-current potentials in a large membrane channel: a simple theory accounts for complex behavior, Biophys. J. 65 (1993) 1093–1100.
[31] E.M. Krammer, F. Homblé, M. Prévost, Concentration dependent ion selectivity in VDAC: a molecular dynamics simulation study, PLoS One 6 (2011) e27994.
[32] E.-M. Krammer, H. Saidani, M. Prévost, F. Homblé, Origin of ion selectivity in Phaseolus coccineus mitochondrial VDAC, Mitochondrion (2014) [http://dx.doi.org/10.1016/j.mito.2014.04.003 (in press)].
[33] P. Ramirez, S. Mafe, V.M. Aguilella, A. Alcaraz, Synthetic nanopores with fixed charges: an electrodiffusion model for ionic transport, Phys. Rev. E Stat. Nonlin. Soft Matter Phys. 68 (2003) 11910.
[34] N. Lakshminaraynaiah, Equations of membrane biophysics, Academic Press, New York, 1984.
[35] O.V. Krasilnikov, R.Z. Sabirov, V.I. Ternovsky, P.G. Merzliak, J.N. Muratkhodjaev, A simple method for the determination of the pore radius of ion channels in planar lipid bilayer membranes, FEMS Microbiol. Lett. 105 (1992) 93–100.
[36] P.G. Merzlyak, L.N. Yuldasheva, C.G. Rodrigues, C.M. Carneiro, O.V. Krasilnikov, S.M. Bezrukov, Polymeric nonelectrolytes to probe pore geometry: application to the alpha-toxin transmembrane channel, Biophys. J. 77 (1999) 3023–3033.
[37] I. Bárcena-Uribarri, M. Thein, E. Maier, M. Bonde, S. Bergström, R. Benz, Use of non-electrolytes reveals the channel size and oligomeric constitution of the Borrelia burgdorferi P66 porin, PLoS One 8 (2013) e78272.
[38] S.M. Bezrukov, I. Vodyanoy, Probing alamethicin channels with water-soluble polymers Effect on conductance of channel states, Biophys. J. 64 (1993) 16–25.
[39] Y.A. Kaulin, L.V. Schagina, S.M. Bezrukov, V.V. Malev, A.M. Feigin, J.Y. Takemoto, J.H. Teeter, J.G. Brand, Cluster Organization of Ion Channels Formed by the Antibiotic Syringomycin E in Bilayer Lipid Membranes, Biophys. J. 74 (1998) 2918–2925.
[40] S.M. Bezrukov, I. Vodyanoy, R.A. Brutyan, J.J. Kasianowicz, Dynamics and Free Energy of Polymers Partitioning into a Nanoscale Pore, Macromolecules 29 (1996) 8517–8522.
[41] T.K. Rostovtseva, E.M. Nestorovich, S.M. Bezrukov, Partitioning of Differently Sized Poly(ethylene glycol)s into OmpF Porin, Biophys. J. 82 (2002) 160–169.
[42] V.C. Simonet, A. Basle, K.E. Klose, A.H. Delcour, The Vibrio cholerae porins OmpU and OmpT have distinct channel properties, J. Biol. Chem. 278 (2003) 17539–17545.
[43] G. Duret, A.H. Delcour, Deoxycholic acid blocks vibrio cholerae OmpT but not OmpU porin, J. Biol. Chem. 281 (2006) 19899–19905.
[44] G. Duret, V. Simonet, A.H. Delcour, Modulation of Vibrio cholerae porin function by acidic pH, Channels (Austin) 1 (2007) 70–79.
[45] G. Duret, A.H. Delcour, Size and dynamics of the Vibrio cholerae porins OmpU and OmpT probed by polymer exclusion, Biophys. J. 98 (2010) 1820–1829.
[46] J. Tommassen, B. Lugtenberg, Outer membrane protein e of Escherichia coli K-12 is co-regulated with alkaline phosphatase, J. Bacteriol. 143 (1980) 151–157.
[47] N. Overbeeke, B. Lugtenberg, Expression of outer membrane protein e of escherichia coli K12 by phosphate limitation, FEBS Lett. 112 (1980) 229–232.
[48] K. Poole, R.E. Hancock, Phosphate-starvation-induced outer membrane proteins of members of the families Enterobacteriaceae and Pseudomonodaceae: demonstration of immunological cross-reactivity with an antiserum specific for porin protein P of Pseudomonas aeruginosa, J. Bacteriol. 165 (1986) 987–993.
[49] R.E. Hancock, K. Poole, R. Benz, Outer membrane protein P of Pseudomonas aeruginosa: regulation by phosphate deficiency and formation of small anion-specific channels in lipid bilayer membranes, J. Bacteriol. 150 (1982) 730–738.
[50] R. Benz, R.P. Darveau, R.E.W. Hancock, Outer-membrane protein PhoE from Escherichia coli forms anion-selective pores in lipid-bilayer membranes, Eur. J. Biochem. 140 (1984) 319–324.
[51] R. Benz, A. Schmid, R.E. Hancock, Ion selectivity of gram-negative bacterial porins, J. Bacteriol. 162 (1985) 722–727.
[52] K. Bauer, P. van der Ley, R. Benz, J. Tommassen, The pho-controlled outer membrane porin PhoE does not contain specific binding sites for phosphate or polyphosphates, J. Biol. Chem. 263 (1988) 13046–13053.
[53] R.E. Hancock, R. Benz, Demonstration and chemical modification of a specific phosphate binding site in the phosphate-starvation-inducible outer membrane porin protein P of Pseudomonas aeruginosa, Biochim. Biophys. Acta 860 (1986) 699–707.
[54] R. Benz, R.E. Hancock, Mechanism of ion transport through the anion-selective channel of the Pseudomonas aeruginosa outer membrane, J. Gen. Physiol. 89 (1987) 275–295.
[55] R. Benz, C. Egli, R.E.W. Hancock, Anion transport through the phosphate-specific OprP-channel of the Pseudomonas aeruginosa outer membrane: Effects of phosphate, di- and tribasic anions and of negatively-charged lipids, Biochim. Biophys. Acta Biomembr. 1149 (1993) 224–230.
[56] M.L. Lopez, M. Aguilella-Arzo, V.M. Aguilella, A. Alcaraz, Ion selectivity of a biological channel at high concentration ratio: insights on small ion diffusion and binding, J. Phys. Chem. B 113 (2009) 8745–8751.
[57] C. Danelon, A. Suenaga, M. Winterhalter, I. Yamato, Molecular origin of the cation selectivity in OmpF porin: single channel conductances vs free energy calculation, Biophys. Chem. 104 (2003) 591–603.
[58] P.S. Phale, A. Philippsen, C. Widmer, V.P. Phale, J.P. Rosenbusch, T. Schirmer, Role of charged residues at the OmpF porin channel constriction probed by mutagenesis and simulation, Biochemistry 40 (2001) 6319–6325.
[59] W. Im, B. Roux, Ions and counterions in a biological channel: a molecular dynamics simulation of OmpF porin from Escherichia coli in an explicit membrane with 1 M KCl aqueous salt solution, J. Mol. Biol. 319 (2002) 1177–1197.
[60] Y. Koyabashi, T. Akae, The mechanism of ion selectivity of OmpF-porin pores of Escherichia coli, Eur. J. Biochem. 151 (1985) 231–236.
[61] F. Fornasiero, J.B. In, S. Kim, H.G. Park, Y. Wang, C.P. Grigoropoulos, A. Noy, O. Bakajin, pH-tunable ion selectivity in carbon nanotube pores, Langmuir 26 (2010) 14848–14853.
[62] P. Läuger, Ion transport through pores: A rate-theory analysis, Biochim. Biophys. Acta Biomembr. 311 (1973) 423–441.